



planck

Non-Gaussianity results from Planck

Bartjan van Tent

Laboratoire de Physique Théorique, Orsay (Paris-Sud)

On behalf of the Planck collaboration

*Planck 2013 Results. XXIV. Constraints on primordial non-Gaussianity,
arXiv:1303.5084*



The scientific results that we present today are a product of the Planck Collaboration, including individuals from more than 100 scientific institutes in Europe, the USA and Canada



Planck is a project of the European Space Agency, with instruments provided by two scientific Consortia funded by ESA member states (in particular the lead countries: France and Italy) with contributions from NASA (USA), and telescope reflectors provided in a collaboration between ESA and a scientific Consortium led and funded by Denmark.



Outline

- 1. Introduction and motivation:**
why look for non-Gaussianity, predictions from inflation
- 2. Observing non-Gaussianity in the CMB:**
bispectrum, templates, estimators
- 3. Results and validation:**
 f_{NL} results, dependence on ℓ , consistency, smoothed bispectrum, isocurvature non-Gaussianity
- 4. Conclusions and outlook**



1. Introduction and motivation

Beyond linear perturbation theory: **non-Gaussianity**

CMB observations are becoming accurate enough to go beyond linear approx.:

- ▶ All inflation models: **non-linear** effects (potential, gravity)
→ **non-Gaussianity**.
- ▶ New way to constrain and discriminate between inflation models using **CMB** observations.
- ▶ Need **formalism** to describe production & evolution non-linear pert.:
 δN , *long wavelength*, ...
- ▶ Need **estimator** to extract NG information from the CMB data:
KSW, *binned*, *modal*, ...



(Local) non-Gaussianity from inflation:

Linear: $\hat{\phi}_L = \phi_L \hat{a}^\dagger + \phi_L^* \hat{a} \Rightarrow$ **Gaussian**, $\langle \hat{\phi} \hat{\phi} \hat{\phi} \rangle = 0$.

Non-linear: $\hat{\phi} = \hat{\phi}_L + f_{\text{NL}} (\hat{\phi}_L^2 - \langle \hat{\phi}_L^2 \rangle)$

\Rightarrow **non-Gaussian**: $\langle \hat{\phi} \hat{\phi} \hat{\phi} \rangle \sim f_{\text{NL}} \langle \hat{\phi}_L \hat{\phi}_L \hat{\phi}_L \hat{\phi}_L \rangle \sim f_{\text{NL}} \langle \hat{\phi}_L^2 \rangle^2$

Hence f_{NL} can be viewed as the amplitude of the bispectrum (3-pt correlator) divided by the power spectrum (2-pt correlator) squared.



(Local) non-Gaussianity from inflation:

Linear: $\hat{\phi}_L = \phi_L \hat{a}^\dagger + \phi_L^* \hat{a} \Rightarrow$ **Gaussian**, $\langle \hat{\phi} \hat{\phi} \hat{\phi} \rangle = 0$.

Non-linear: $\hat{\phi} = \hat{\phi}_L + f_{NL} (\hat{\phi}_L^2 - \langle \hat{\phi}_L^2 \rangle)$

\Rightarrow **non-Gaussian**: $\langle \hat{\phi} \hat{\phi} \hat{\phi} \rangle \sim f_{NL} \langle \hat{\phi}_L \hat{\phi}_L \hat{\phi}_L \hat{\phi}_L \rangle \sim f_{NL} \langle \hat{\phi}_L^2 \rangle^2$

Hence f_{NL} can be viewed as the amplitude of the bispectrum (3-pt correlator) divided by the power spectrum (2-pt correlator) squared.

Note: $\phi \sim 10^{-5} \Rightarrow$ almost-Gaussianity prediction of inflation confirmed to 10^{-4} !
(cf. flatness to 10^{-3})

Theoretical expectations:

- Single-field slow-roll inflation: $f_{NL} \sim 10^{-2}$ [Maldacena, astro-ph/0210603]
- Non-linear effects at recombination: $f_{NL} \sim 1$ [Huang & Vernizzi, arXiv:1212.3573]
- Multiple-field inflation / curvaton models / modified vacua / non-standard kinetic terms / inflation alternatives: $f_{NL} \lesssim 100$

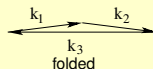
[Bartolo, Matarrese, Riotto, Rigopoulos, Shellard, BvT, Tzavara, Sasaki, Byrnes, Vernizzi, Wands, Bernardeau, Uzan, Renaux-Petel, Langlois, Lyth, Malik, Van der Schaar, Jackson, Enqvist, Nurmi, Tolley, Lehnert, Barnaby, Mizuno, ...]



Predictions from inflation

- ▶ **Local**: created on super-horizon scales during or after inflation in the presence of multiple fields (transfer from isocurvature to adiabatic mode). Peaks on squeezed configurations ($k_1 \ll k_2 \approx k_3$).

$$B^{\text{local}}(k_1, k_2, k_3) = 2[P_{k_1} P_{k_2} + P_{k_1} P_{k_3} + P_{k_2} P_{k_3}].$$





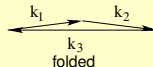
Predictions from inflation

- ▶ **Local**: created on super-horizon scales during or after inflation in the presence of multiple fields (transfer from isocurvature to adiabatic mode). Peaks on squeezed configurations ($k_1 \ll k_2 \approx k_3$).

$$B^{\text{local}}(k_1, k_2, k_3) = 2[P_{k_1} P_{k_2} + P_{k_1} P_{k_3} + P_{k_2} P_{k_3}].$$

- ▶ **Equilateral**: created at horizon-crossing in single-field inflation with non-standard kinetic terms. Peaks on equilateral configurations ($k_1 \approx k_2 \approx k_3$).

$$B^{\text{equil}}(k_1, k_2, k_3) = 6\{-[P_{k_1} P_{k_2} + 2 \text{ perm.}] - 2P_{k_1}^{2/3} P_{k_2}^{2/3} P_{k_3}^{2/3} + [P_{k_1} P_{k_2}^{2/3} P_{k_3}^{1/3} + 5 \text{ perm.}]\}.$$





Predictions from inflation

- ▶ **Local**: created on super-horizon scales during or after inflation in the presence of multiple fields (transfer from isocurvature to adiabatic mode). Peaks on squeezed configurations ($k_1 \ll k_2 \approx k_3$).

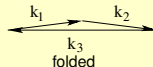
$$B^{\text{local}}(k_1, k_2, k_3) = 2[P_{k_1} P_{k_2} + P_{k_1} P_{k_3} + P_{k_2} P_{k_3}].$$

- ▶ **Equilateral**: created at horizon-crossing in single-field inflation with non-standard kinetic terms. Peaks on equilateral configurations ($k_1 \approx k_2 \approx k_3$).

$$B^{\text{equil}}(k_1, k_2, k_3) = 6\{-[P_{k_1} P_{k_2} + 2 \text{ perm.}] - 2P_{k_1}^{2/3} P_{k_2}^{2/3} P_{k_3}^{2/3} + [P_{k_1} P_{k_2}^{2/3} P_{k_3}^{1/3} + 5 \text{ perm.}]\}.$$

- ▶ **Folded**: created in models with excited initial states (non-Bunch-Davies vacua). Peaks on flat configurations ($k_1 \approx k_2 \approx k_3/2$).

$$B^{\text{flat}}(k_1, k_2, k_3) = 6\{[P_{k_1} P_{k_2} + 2 \text{ perm.}] + 3P_{k_1}^{2/3} P_{k_2}^{2/3} P_{k_3}^{2/3} - [P_{k_1} P_{k_2}^{2/3} P_{k_3}^{1/3} + 5 \text{ perm.}]\}.$$





Predictions from inflation

- ▶ **Local**: created on super-horizon scales during or after inflation in the presence of multiple fields (transfer from isocurvature to adiabatic mode). Peaks on squeezed configurations ($k_1 \ll k_2 \approx k_3$).

$$B^{\text{local}}(k_1, k_2, k_3) = 2[P_{k_1} P_{k_2} + P_{k_1} P_{k_3} + P_{k_2} P_{k_3}].$$

- ▶ **Equilateral**: created at horizon-crossing in single-field inflation with non-standard kinetic terms. Peaks on equilateral configurations ($k_1 \approx k_2 \approx k_3$).

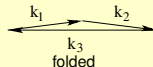
$$B^{\text{equil}}(k_1, k_2, k_3) = 6\{-[P_{k_1} P_{k_2} + 2 \text{ perm.}] - 2P_{k_1}^{2/3} P_{k_2}^{2/3} P_{k_3}^{2/3} + [P_{k_1} P_{k_2}^{2/3} P_{k_3}^{1/3} + 5 \text{ perm.}]\}.$$

- ▶ **Folded**: created in models with excited initial states (non-Bunch-Davies vacua). Peaks on flat configurations ($k_1 \approx k_2 \approx k_3/2$).

$$B^{\text{flat}}(k_1, k_2, k_3) = 6\{[P_{k_1} P_{k_2} + 2 \text{ perm.}] + 3P_{k_1}^{2/3} P_{k_2}^{2/3} P_{k_3}^{2/3} - [P_{k_1} P_{k_2}^{2/3} P_{k_3}^{1/3} + 5 \text{ perm.}]\}.$$

- ▶ **Orthogonal**: combination of equilateral and folded shape, constructed to be orthogonal to equilateral template. Generic (non-standard) single-field models produce linear combination of equilateral and orthogonal.

$$B^{\text{ortho}}(k_1, k_2, k_3) = 6\{-3[P_{k_1} P_{k_2} + 2 \text{ perm.}] - 8P_{k_1}^{2/3} P_{k_2}^{2/3} P_{k_3}^{2/3} + 3[P_{k_1} P_{k_2}^{2/3} P_{k_3}^{1/3} + 5 \text{ perm.}]\}.$$





In this talk we will only consider the **local**, **equilateral**, and **orthogonal** primordial templates (since folded is not independent).

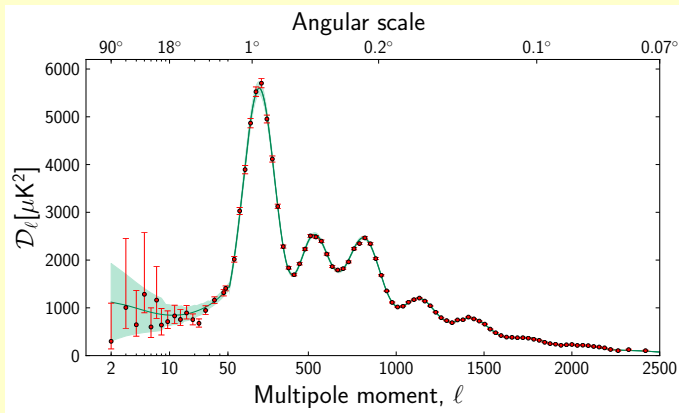
Note that these are all **separable approximations** to classes of similar bispectra. For a first investigation it is useful to limit the number of shapes, and separability is also a requirement for the KSW estimator.

However, with the newer estimators (binned, modal) separability is no longer required. We also tested **additional templates**: several specific inflation model shapes, as well as many feature and resonant models (parametrized by a period k_c and a phase ϕ). → see *Paul Shellard's talk*



2. Observing non-Gaussianity in the CMB

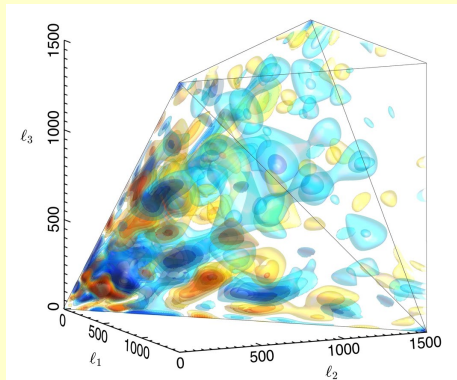
CMB 2-pt correlation function $\langle T(\Omega_1)T(\Omega_2) \rangle \Rightarrow$ Power spectrum C_ℓ



$$T(\Omega) = \sum_{\ell=2}^{\infty} \sum_{m=-\ell}^{+\ell} a_{\ell m} Y_{\ell m}(\Omega); \quad C_\ell = \frac{1}{2\ell+1} \sum_{m=-\ell}^{+\ell} |a_{\ell m}|^2; \quad D_\ell = \frac{\ell(\ell+1)C_\ell}{2\pi}$$



CMB 3-pt correlation function $\langle T(\Omega_1)T(\Omega_2)T(\Omega_3) \rangle \Rightarrow$ bispectrum $B_{\ell_1\ell_2\ell_3}$



$$\begin{aligned}
 B_{\ell_1\ell_2\ell_3} &= \sqrt{\frac{(2\ell_1+1)(2\ell_2+1)(2\ell_3+1)}{4\pi}} \begin{pmatrix} \ell_1 & \ell_2 & \ell_3 \\ 0 & 0 & 0 \end{pmatrix} \sum_{m_1, m_2, m_3} \begin{pmatrix} \ell_1 & \ell_2 & \ell_3 \\ m_1 & m_2 & m_3 \end{pmatrix} a_{\ell_1 m_1} a_{\ell_2 m_2} a_{\ell_3 m_3} \\
 &= \int d\Omega T_{\ell_1}(\Omega) T_{\ell_2}(\Omega) T_{\ell_3}(\Omega) \quad \text{with} \quad T_{\ell}(\Omega) = \sum_m a_{\ell m} Y_{\ell m}(\Omega)
 \end{aligned}$$



We searched explicitly for 5 types of bispectrum with templates $B^{th,(i)}$ and amplitudes $f_{NL}^{(i)}$, where $i = 1, \dots, 5$. We did:

- Fully joint analysis where all 5 are assumed present, $B_{\ell_1 \ell_2 \ell_3} = \sum_{i=1}^5 f_{NL}^{(i)} B_{\ell_1 \ell_2 \ell_3}^{th,(i)}$;
- Fully independent analysis where only 1 is assumed present;
- Various intermediate cases (e.g. 1 primordial + foregrounds).

▶ 3 primordial shapes: local, equilateral, and orthogonal

$$B_{\ell_1 \ell_2 \ell_3}^{th,(i)} \sim \int r^2 dr \int k_1^2 dk_1 \int k_2^2 dk_2 \int k_3^2 dk_3 \Delta_{\ell_1}(k_1) \Delta_{\ell_2}(k_2) \Delta_{\ell_3}(k_3) j_{\ell_1}(k_1 r) j_{\ell_2}(k_2 r) j_{\ell_3}(k_3 r) B^{(i)}(k_1, k_2, k_3)$$

with $\Delta_{\ell}(k)$ radiation transfer function and $B^{(i)}(k_1, k_2, k_3)$ primordial bispectrum

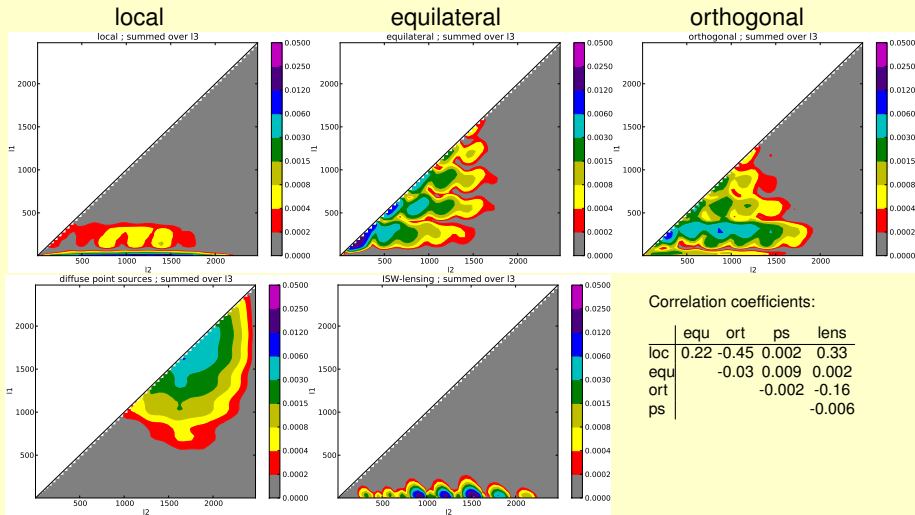
▶ 2 non-primordial shapes:

- Bispectrum due to diffuse (non-resolved) extra-galactic **point sources** (Poisson distribution): peaks on high- ℓ equilateral configurations (since it is intrinsically constant $B_{\ell_1 \ell_2 \ell_3}^{PS} \sim \text{const}$). [Komatsu, Spergel, astro-ph/0005036]
- Bispectrum due to the correlation between the integrated Sachs-Wolfe (**ISW**) effect and gravitational **lensing**: peaks on squeezed configurations. [Goldberg, Spergel, astro-ph/9811251; Lewis et al., arXiv:1101.2234]

$$B_{\ell_1 \ell_2 \ell_3}^{\text{lensISW}} \sim [\ell_2(\ell_2 + 1) + \ell_3(\ell_3 + 1) - \ell_1(\ell_1 + 1)] \left(C_{\ell_2}^{T\psi} C_{\ell_3} + C_{\ell_3}^{T\psi} C_{\ell_2} \right) + 2 \text{ perm.}$$



Relative weight of the different templates in ℓ_1 - ℓ_2 space, summed over ℓ_3 ($\ell_1 \leq \ell_2 \leq \ell_3$). The colour scale is logarithmic.



Correlation coefficients:

	equ	ort	ps	lens
loc	0.22	-0.45	0.002	0.33
equ		-0.03	0.009	0.002
ort			-0.002	-0.16
ps				-0.006

point sources

ISW-lensing



Optimal f_{NL} estimator

$$\hat{f}_{\text{NL}} = \frac{1}{F} \sum_{\ell_1 \leq \ell_2 \leq \ell_3} \frac{(B_{f_{\text{NL}}=1}^{\text{th}})^{\cancel{f}}}{\text{Var}_G(B^{\text{obs}})} \frac{B^{\text{obs}}}{B_{f_{\text{NL}}=1}^{\text{th}}}$$

$$\text{where } F = \frac{1}{\text{Var}_G(\hat{f}_{\text{NL}})} = \chi^2_{(f_{\text{NL}}=1)} = \sum_{\ell_1 \leq \ell_2 \leq \ell_3} \frac{(B_{f_{\text{NL}}=1}^{\text{th}})^2}{\text{Var}_G(B^{\text{obs}})}$$

$$\text{Var}_G(B^{\text{obs}}) \sim (b_{\ell_1}^2 C_{\ell_1} + N_{\ell_1})(b_{\ell_2}^2 C_{\ell_2} + N_{\ell_2})(b_{\ell_3}^2 C_{\ell_3} + N_{\ell_3}), \quad b_{\ell} = \text{beam}, N_{\ell} = \text{noise}$$



Optimal f_{NL} estimator

$$\hat{f}_{\text{NL}} = \frac{1}{F} \sum_{\ell_1 \leq \ell_2 \leq \ell_3} \frac{(B_{f_{\text{NL}}=1}^{\text{th}})^{\cancel{f}}}{\text{Var}_G(B^{\text{obs}})} \frac{B^{\text{obs}}}{B_{f_{\text{NL}}=1}^{\text{th}}}$$

$$\text{where } F = \frac{1}{\text{Var}_G(\hat{f}_{\text{NL}})} = \chi^2_{(f_{\text{NL}}=1)} = \sum_{\ell_1 \leq \ell_2 \leq \ell_3} \frac{(B_{f_{\text{NL}}=1}^{\text{th}})^2}{\text{Var}_G(B^{\text{obs}})}$$

$$\text{Var}_G(B^{\text{obs}}) \sim (b_{\ell_1}^2 C_{\ell_1} + N_{\ell_1})(b_{\ell_2}^2 C_{\ell_2} + N_{\ell_2})(b_{\ell_3}^2 C_{\ell_3} + N_{\ell_3}), \quad b_{\ell} = \text{beam}, N_{\ell} = \text{noise}$$

Remarks:

- ▶ The theoretically optimal estimator should not use the above approximation for the variance, but use full inverse covariance weighting. In practice for the Planck analysis the above expression also gives optimal results, if the masked parts of the map have been filled in using a simple diffusive inpainting scheme (replacing each masked pixel with the average of its 8 neighbours, iteratively).



Optimal f_{NL} estimator

$$\hat{f}_{\text{NL}} = \frac{1}{F} \sum_{\ell_1 \leq \ell_2 \leq \ell_3} \frac{(B_{f_{\text{NL}}=1}^{\text{th}})^{\cancel{2}} B^{\text{obs}}}{\text{Var}_G(B^{\text{obs}}) \cancel{B_{f_{\text{NL}}=1}^{\text{th}}}}$$

$$\text{where } F = \frac{1}{\text{Var}_G(\hat{f}_{\text{NL}})} = \chi^2_{(f_{\text{NL}}=1)} = \sum_{\ell_1 \leq \ell_2 \leq \ell_3} \frac{(B_{f_{\text{NL}}=1}^{\text{th}})^2}{\text{Var}_G(B^{\text{obs}})}$$

$\text{Var}_G(B^{\text{obs}}) \sim (b_{\ell_1}^2 C_{\ell_1} + N_{\ell_1})(b_{\ell_2}^2 C_{\ell_2} + N_{\ell_2})(b_{\ell_3}^2 C_{\ell_3} + N_{\ell_3})$, b_{ℓ} = beam, N_{ℓ} = noise

Remarks:

- ▶ The theoretically optimal estimator should not use the above approximation for the variance, but use full inverse covariance weighting. In practice for the Planck analysis the above expression also gives optimal results, if the masked parts of the map have been filled in using a simple diffusive inpainting scheme (replacing each masked pixel with the average of its 8 neighbours, iteratively).
- ▶ When rotational invariance is broken due to the presence of a mask and anisotropic noise, optimality is restored by adding a linear correction term:

$B_{\ell_1 \ell_2 \ell_3}^{\text{obs}} \rightarrow B_{\ell_1 \ell_2 \ell_3}^{\text{obs}} - B_{\ell_1 \ell_2 \ell_3}^{\text{lin}}$ with $B_{\ell_1 \ell_2 \ell_3}^{\text{lin}} = \int d\Omega [T_{\ell_1}(\Omega) \langle T_{\ell_2}^G(\Omega) T_{\ell_3}^G(\Omega) \rangle + 2 \text{ perms}]$
 where the T_{ℓ}^G are simulated Gaussian maps. [Creminelli et al., astro-ph/0509029]

- ▶ For a joint analysis of multiple templates the expression becomes:

$$\hat{f}_{\text{NL}}^{(i)} = \sum_j (F^{-1})^{ij} \sum B^{\text{th},(j)} B^{\text{obs}} / \text{Var}_G(B^{\text{obs}}) \quad \text{with} \quad F^{ij} = \sum B^{\text{th},(i)} B^{\text{th},(j)} / \text{Var}_G(B^{\text{obs}})$$



$$\hat{f}_{\text{NL}} = \frac{1}{F} \sum_{\ell_1 \leq \ell_2 \leq \ell_3} \frac{B_{\ell_1 \ell_2 \ell_3}^{\text{th}} B^{\text{obs}}}{\text{Var}_G(B^{\text{obs}})}$$

Computing the optimal estimator explicitly in the most general case is computationally too expensive ($\mathcal{O}(1\text{e}9)$ computations of $B_{\ell_1 \ell_2 \ell_3}^{\text{obs}}$ per map)

⇒ need some approximations and/or assumptions

⇒ different estimators (= different implementations of optimal estimator)

- ▶ **KSW** estimator [Komatsu, Spergel, Wandelt, *astro-ph/0305189*]
- ▶ **binned** estimator [Bucher, BvT, Carvalho, *arXiv:0911.1642*]
- ▶ **modal** estimator [Fergusson, Liguori, Shellard, *arXiv:0912.5516*] → see Paul Shellard's talk

Also checked results with wavelet estimator (current implementation not yet optimal) and Minkowski functional estimator (suboptimal for bispectrum).



KSW estimator

[Komatsu, Spergel, Wandelt, astro-ph/0305189]

$$\hat{f}_{\text{NL}} = \frac{1}{F} \sum_{\ell_1 \leq \ell_2 \leq \ell_3} \frac{B_{\text{fNL}=1}^{\text{th}} B^{\text{obs}}}{\text{Var}_G(B^{\text{obs}})}$$

$$B_{\ell_1 \ell_2 \ell_3}^{\text{obs}} = \int d\Omega T_{\ell_1}(\Omega) T_{\ell_2}(\Omega) T_{\ell_3}(\Omega)$$

$$\text{Var}_G(B^{\text{obs}}) \sim (b_{\ell_1}^2 C_{\ell_1} + N_{\ell_1})(b_{\ell_2}^2 C_{\ell_2} + N_{\ell_2})(b_{\ell_3}^2 C_{\ell_3} + N_{\ell_3})$$

$$B_{\ell_1 \ell_2 \ell_3}^{\text{th}} \sim \int r^2 dr \int k_1^2 dk_1 \int k_2^2 dk_2 \int k_3^2 dk_3 \Delta_{\ell_1}(k_1) \Delta_{\ell_2}(k_2) \Delta_{\ell_3}(k_3) j_{\ell_1}(k_1 r) j_{\ell_2}(k_2 r) j_{\ell_3}(k_3 r) B(k_1, k_2, k_3)$$

Assumptions/approximations for KSW:

- ▶ Bispectrum templates are all **separable**:
 $B(k_1, k_2, k_3) = \alpha_1(k_1)\alpha_2(k_2)\alpha_3(k_3) + \text{perms}$
- ▶ Integral over r can be computed with relatively few points

$$\Rightarrow \hat{f}_{\text{NL}} \sim \int r^2 dr \int d\Omega \left[\sum_{\ell_1} \frac{\int k_1^2 dk_1 \Delta_{\ell_1}(k_1) j_{\ell_1}(k_1 r) \alpha_1(k_1) T_{\ell_1}(\Omega)}{b_{\ell_1}^2 C_{\ell_1} + N_{\ell_1}} \right] \left[1 \rightarrow 2 \right] \left[1 \rightarrow 3 \right]$$

KSW estimator only provides single number f_{NL} , no full bispectrum reconstruction. Partially mitigated by Skew- C_ℓ extension [Munshi, Heavens, arXiv:0904.4478].



Binned bispectrum estimator: 1) f_{NL}

[M.Bucher, BvT, C.Carvalho, arXiv:0911.1642]

$$\hat{f}_{NL} = \frac{1}{F} \sum_{\ell_1 \leq \ell_2 \leq \ell_3} \frac{B_{f_{NL}=1}^{th} B^{obs}}{\text{Var}_G(B^{obs})} \Rightarrow \text{Binning in } \ell\text{-space}$$

$$\Rightarrow \hat{f}_{NL} \approx \frac{1}{F^{binned}} \sum_{\substack{\text{bins} \\ \ell_1 \leq \ell_2 \leq \ell_3}} \left(\frac{\sum_{\ell_1, \ell_2, \ell_3 \in \text{bin}} B_{f_{NL}=1}^{th} \sum_{\ell_1, \ell_2, \ell_3 \in \text{bin}} B^{obs}}{\sum_{\ell_1, \ell_2, \ell_3 \in \text{bin}} \text{Var}_G(B^{obs})} \right)$$

with $\sum_{\ell_1, \ell_2, \ell_3 \in \text{bin}} B^{obs} = \int d\Omega T_{\Delta\ell_1} T_{\Delta\ell_2} T_{\Delta\ell_3}$ where $T_{\Delta\ell}(\Omega) = \sum_{\ell \in \text{bin}} \sum_m a_{\ell m} Y_{\ell m}(\Omega)$.

One determines the optimal binning by maximizing the correlation between the binned and the exact template.

Using 51 bins (continuous but unequal-size) at Planck resolution ($\ell_{max} = 2500$) gives $\geq 99\%$ correlation for e.g. local and equilateral.



Binned bispectrum estimator

$$\hat{f}_{\text{NL}} \approx \frac{1}{F_{\text{binned}}} \sum_{\substack{\text{bins} \\ i_1 \leq i_2 \leq i_3}} \left(\frac{\sum_{\ell_1, \ell_2, \ell_3 \in \text{bin}} B_{f_{\text{NL}}=1}^{\text{th}} \sum_{\ell_1, \ell_2, \ell_3 \in \text{bin}} B^{\text{obs}}}{\sum_{\ell_1, \ell_2, \ell_3 \in \text{bin}} \text{Var}_G(B^{\text{obs}})} \right)$$

Advantages:

- ▶ Fast on a single map.
- ▶ **Theoretical** template does not need to be separable.
- ▶ **Theoretical** and **observational** part computed and saved separately, only combined in final sum over bins (which takes just seconds to compute) \Rightarrow
 - ▶ No need to rerun maps to determine e.g. f_{NL} for an additional template.
 - ▶ **Full (binned) bispectrum** is direct output of code.
- ▶ Easy to investigate dependence on ℓ by leaving out bins from final sum.

Disadvantages:

- ▶ **Theoretical** template must not change too much over a bin (OK for local, equilateral, orthogonal, point sources; a bit less for ISW-lensing).
- ▶ (Current implementation) Linear term cannot be precomputed, so computation time scales linearly with number of maps.



3. Results and validation

	Independent			ISW-lensing subtracted		
	KSW	Binned	Modal	KSW	Binned	Modal
SMICA						
Local	9.8 ± 5.8	9.2 ± 5.9	8.3 ± 5.9	2.7 ± 5.8	2.2 ± 5.9	1.6 ± 6.0
Equilateral	-37 ± 75	-20 ± 73	-20 ± 77	-42 ± 75	-25 ± 73	-20 ± 77
Orthogonal	-46 ± 39	-39 ± 41	-36 ± 41	-25 ± 39	-17 ± 41	-14 ± 42
NILC						
Local	11.6 ± 5.8	10.5 ± 5.8	9.4 ± 5.9	4.5 ± 5.8	3.6 ± 5.8	2.7 ± 6.0
Equilateral	-41 ± 76	-31 ± 73	-20 ± 76	-48 ± 76	-38 ± 73	-20 ± 78
Orthogonal	-74 ± 40	-62 ± 41	-60 ± 40	-53 ± 40	-41 ± 41	-37 ± 43
SEVEM						
Local	10.5 ± 5.9	10.1 ± 6.2	9.4 ± 6.0	3.4 ± 5.9	3.2 ± 6.2	2.6 ± 6.0
Equilateral	-32 ± 76	-21 ± 73	-13 ± 77	-36 ± 76	-25 ± 73	-13 ± 78
Orthogonal	-34 ± 40	-30 ± 42	-24 ± 42	-14 ± 40	-9 ± 42	-2 ± 42
C-R						
Local	12.4 ± 6.0	11.3 ± 5.9	10.9 ± 5.9	6.4 ± 6.0	5.5 ± 5.9	5.1 ± 5.9
Equilateral	-60 ± 79	-52 ± 74	-33 ± 78	-62 ± 79	-55 ± 74	-32 ± 78
Orthogonal	-76 ± 42	-60 ± 42	-63 ± 42	-57 ± 42	-41 ± 42	-42 ± 42

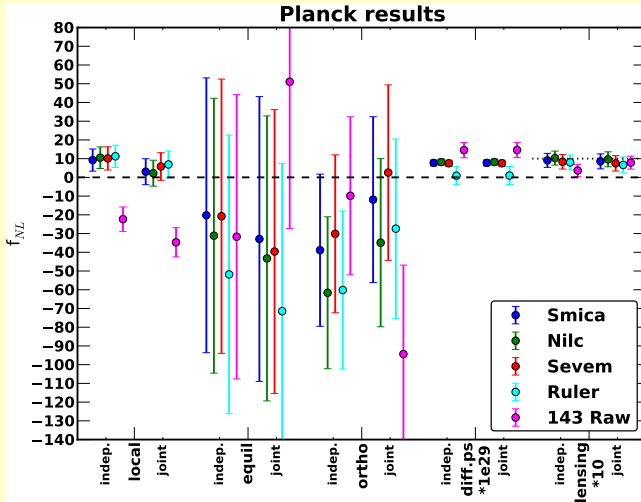
Final Planck results:

$$\text{local: } f_{NL}^{\text{loc}} = 2.7 \pm 5.8$$

$$\text{equil.: } f_{NL}^{\text{equ}} = -42 \pm 75$$

$$\text{ortho.: } f_{NL}^{\text{ort}} = -25 \pm 39$$

Excellent agreement between different estimators and between different component separation methods!

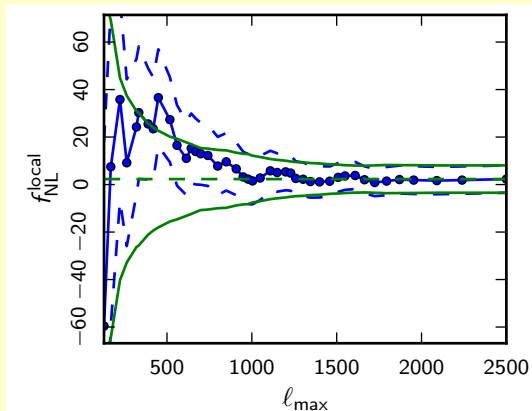


- ▶ No leo primordial NG (when marginalizing/subtracting ISW-lensing)
- ▶ First detection ISW-lensing bispec.
- ▶ Good agreement different component separation methods
- ▶ Point sources in SMICA, NILC, SEVEM; more in Raw 143; not in C-R
- ▶ As expected, foreground contam. in Raw 143 (small mask)

Independent and **fully joint** f_{NL} results (5 shapes) with binned estimator. Results with KSW and modal estimators agree (also wavelets and Mink. funct.).



Dependence on ℓ_{\max} of local f_{NL} (lensing bias subtracted):

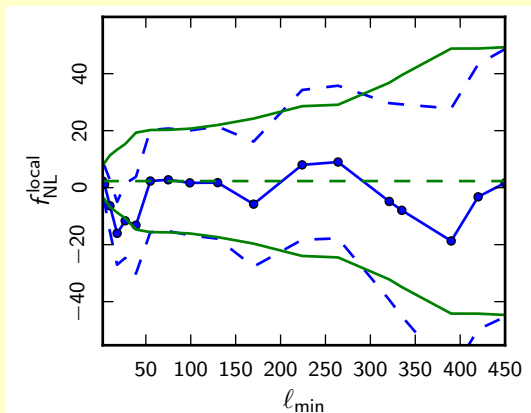


At lower resolution $\ell_{\max} \sim 500$ we recover the WMAP value of around 35, which appears to have been a statistical fluctuation. The final Planck result is driven by the enormous amount of additional data at higher multipoles.

(Result double-checked with KSW estimator.)



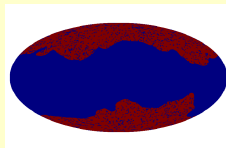
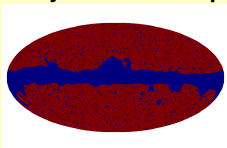
Dependence on ℓ_{\min} of local f_{NL} (lensing bias subtracted):



$f_{\text{NL}}^{\text{loc}}$	independent	lensing bias subtracted
all ℓ_1	9.2 ± 5.8	2.3 ± 5.8
$\ell_1 \leq 54$	9.4 ± 6.0	1.9 ± 6.0
$\ell_1 \geq 55$	4.1 ± 18	2.3 ± 18



Consistency between frequency channels:



	SMICA $f_{\text{sky}} = 0.73$	70 GHz	100 GHz $f_{\text{sky}} = 0.32$	143 GHz	217 GHz
Local	9.2 ± 5.9	19.7 ± 26.0	-2.5 ± 13.2	10.4 ± 9.8	-4.7 ± 9.6
Equilateral	-20 ± 73	159 ± 188	70 ± 132	48 ± 114	-9 ± 114
Orthogonal	-39 ± 39	-78 ± 139	-106 ± 81	-101 ± 64	-84 ± 63

We also checked and confirmed:

- ▶ Consistency when using different masks with the SMICA map;
- ▶ Null results on various jackknife maps (ringhalf, survey, detector set);
- ▶ Negligible impact of SMICA foreground residuals.

All these validation tests were also performed by the modal estimator, further confirming the results.



Binned bispectrum estimator: 2) smoothed bispectrum

Since the binned bispectrum of the map is a direct output of the code, it can be studied explicitly, without any theoretical assumptions (“blind” / **non-parametric**).

To investigate if there is any significant non-Gaussianity in the maps, we consider the bispectrum divided by its expected standard deviation:

$$B_{l_1 l_2 l_3} = \frac{B_{l_1 l_2 l_3}^{\text{obs}}}{\sqrt{\text{Var}_G(B_{l_1 l_2 l_3}^{\text{obs}})}}$$

To bring out coherent features, B is smoothed with a Gaussian kernel with $\sigma = 2$ in bin units.

In the next slides B is shown as a function of l_1 and l_2 , for a given bin in l_3 (which changes with time in the movies). Very red or blue regions indicate significant non-Gaussianity.



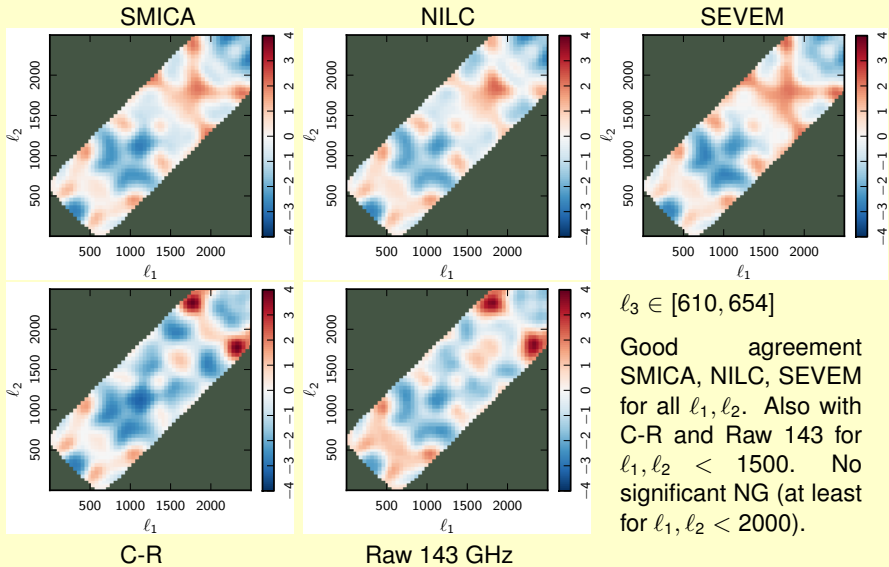
SMICA

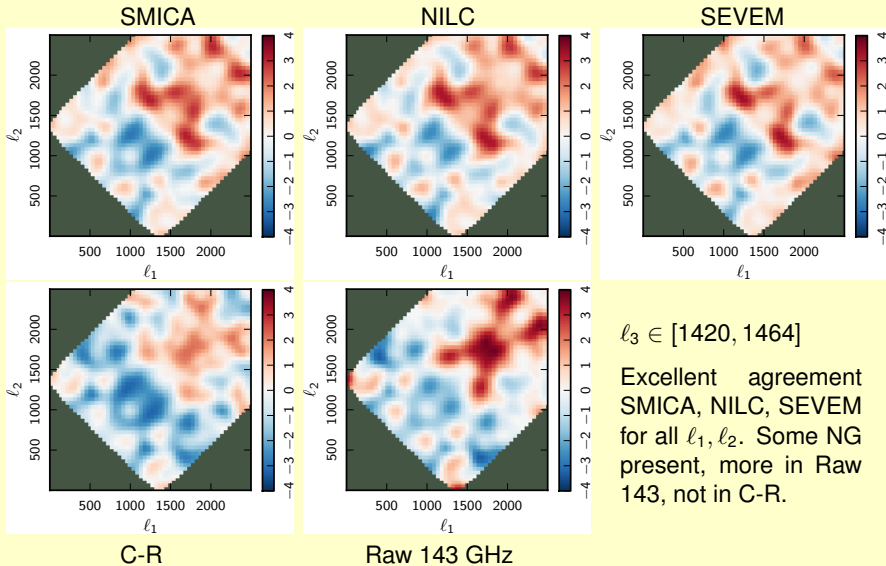
NILC

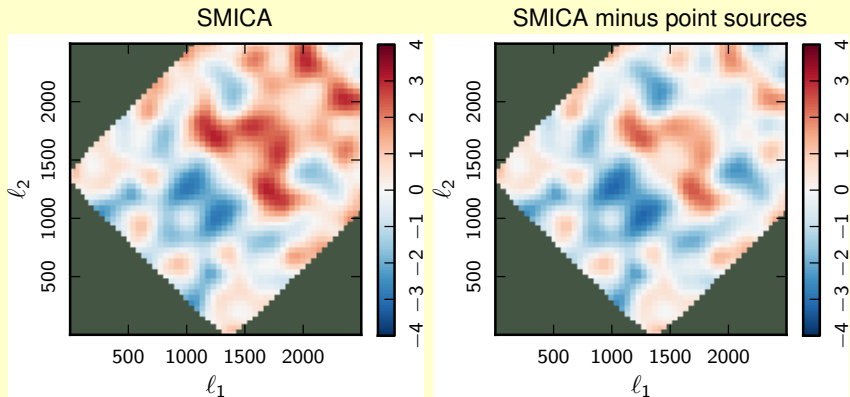
SEVEM

C-R

Raw 143 GHz





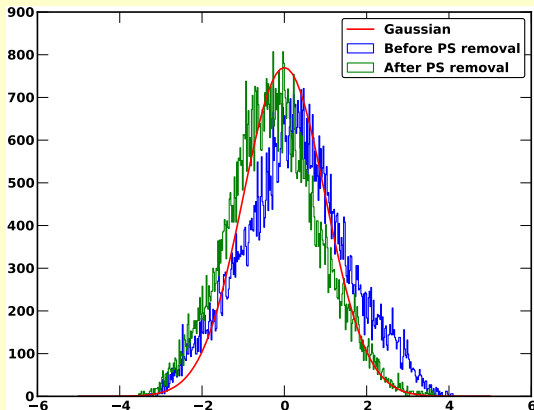


$$l_3 \in [1420, 1464]$$

⇒ The NG signal at high l_1, l_2, l_3 appears to be (mostly) point source contamination (which has negligible correlation with the other templates).

Preliminary more quantitative analysis: *(with Benjamin Racine)*

Map(s)	(max) number bins $\mathcal{B} > 3$ (out of 95687)	Percentage 1e6 sims with larger number
1e6 Gaussian sims	391	-
Smica with PS	1500	0 %
Smica PS removed	216	0.047 %





Isocurvature non-Gaussianity

[Langlois, BvT, arXiv:1104.2567, 1204.5042]

[see also earlier works by Kawasaki, Nakayama, Sekiguchi, Suyama, Takahashi, Hikage]

Assume local primordial bispectrum (I,J,K labels **adiabatic** and **isocurvature** modes):

$$B^{IJK}(k_1, k_2, k_3) = f_{\text{NL}}^{I,JK} P_{\zeta}(k_2) P_{\zeta}(k_3) + f_{\text{NL}}^{J,KI} P_{\zeta}(k_1) P_{\zeta}(k_3) + f_{\text{NL}}^{K,IJ} P_{\zeta}(k_1) P_{\zeta}(k_2)$$

[Produced for example in multiple-field inflation where primordial **adiabatic** and **isocurvature** perturbations X^I can be expressed as

$$X^I = N_a^I \delta\phi^a + \frac{1}{2} N_{ab}^I \delta\phi^a \delta\phi^b + \dots$$

assuming negligible scale dependence of N_a^I and N_{ab}^I .]

Due to symmetries $f_{\text{NL}}^{I,JK} = f_{\text{NL}}^{I,KJ} \Rightarrow$ **6 independent f_{NL} parameters** in the case of 1 **adiabatic** + 1 **isocurvature** mode: $f_{\text{NL}}^{\zeta,\zeta\zeta}$, $f_{\text{NL}}^{\zeta,\zeta S}$, $f_{\text{NL}}^{\zeta,SS}$, $f_{\text{NL}}^{S,\zeta\zeta}$, $f_{\text{NL}}^{S,\zeta S}$, $f_{\text{NL}}^{S,SS}$.

Note: some inflation/curvaton models [Langlois, Lepidi, arXiv:1007.5498] predict a larger isocurvature than adiabatic bispectrum, and at the same time a negligible isocurvature power spectrum.



- Caveats:
- Local shape only, no subtraction of lensing bias.
 - Different convention for f_{NL} defined from ζ , S , not Φ_{adi} , Φ_{iso} .
Hence fully adiabatic case multiplied by 6/5.

Adiabatic + **CDM** isocurvature

	fully indep.	fully joint
a,aa	11 ± 6.9	26 ± 19
a,ac	6.3 ± 4.2	-9.2 ± 12
a,cc	190 ± 120	2300 ± 1200
c,aa	99 ± 180	-250 ± 440
c,ac	77 ± 80	-1900 ± 1400
c,cc	46 ± 120	1100 ± 930

Adiabatic + **neutrino density** isocurvature

	fully indep.	fully joint
a,aa	11 ± 6.9	91 ± 65
a,ad	8.9 ± 6.3	-180 ± 85
a,dd	60 ± 38	1000 ± 680
d,aa	58 ± 34	-180 ± 420
d,ad	42 ± 27	95 ± 870
d,dd	130 ± 96	-740 ± 1200

Adiabatic + **neutrino velocity** isocurvature

	fully indep.	fully joint
a,aa	11 ± 6.9	76 ± 61
a,av	22 ± 13	-290 ± 150
a,vv	71 ± 49	810 ± 530
v,aa	28 ± 18	39 ± 180
v,av	51 ± 28	140 ± 200
v,vv	140 ± 95	-290 ± 610

Note: **Polarization** should reduce these error bars up to a factor 6.



4. Conclusions

- ▶ Models of the early Universe like inflation predict various levels and types of **bispectral non-Gaussianity**.
- ▶ New estimators (**binned, modal**) allow both **parametric** (f_{NL}) and **non-parametric** CMB bispectrum estimation.
- ▶ **Planck f_{NL} results**: no leo primordial NG, much smaller error bars than WMAP, first detection ISW-lensing.
- ▶ **Planck bispectrum reconstruction**: blind tests see mostly point source bispectrum; something more at high ℓ ?
- ▶ **Excellent agreement** between different estimators and component separation methods.
- ▶ Huge amount of **validation tests** confirm robustness of results (dependence on ℓ , on mask, consistency raw and cleaned maps, null tests, foreground residuals, ...).



Outlook

Has Planck killed primordial non-Gaussianity research?



Outlook

Has Planck killed primordial non-Gaussianity research?

No!

- ▶ Computing non-Gaussianity predictions for all early-Universe models, and development of methods to do so, is more important than ever due to tighter constraints from Planck.
- ▶ Current Planck release only gives “definitive” results for generic local, equilateral and orthogonal shapes. Exploration of other shapes is only just starting. Planck might still detect some type of primordial NG!
- ▶ For example: some interesting hints for certain feature models (see Paul Shellard’s talk); some residual NG at high ℓ ?; polarization should improve error bars on isocurvature non-Gaussianity significantly; . . .